Numerical Solution of 3D Unsteady Scattering Problems with Sub-linear Complexity

Sergey Petropavlovsky
National Research University
Higher School of Economics
Moscow 101000, Russia
spetropavlovskij@hse.ru

Semyon Tsynkov
Department of Mathematics
North Carolina State University
Raleigh, NC, USA
https://orcid.org/0000-0003-1069-9612

Eli Turkel
School of Mathematical Sciences
Tel Aviv University
Tel Aviv, Israel
turkel@tauex.tau.ac.il

***Abstract*—We present an efficient high order accurate boundary algorithm for the numerical solution of unsteady exterior initial boundary problems for the three-dimensional wave equation. The algorithm relies on the method of difference potentials combined with the Huygens' principle.**

***Index Terms*—method of difference potentials, Huygens' principle, 3D wave equation.**

I. Introduction

Consider an exterior initial boundary value problem (IBVP) for the three-dimensional homogeneous wave (d'Alembert) equation:

$$\frac{1}{c^2}\frac{\partial^2 u}{\partial t^2} - \Delta u = 0, \quad \text{on} \quad \mathbb{R}^3\backslash\Omega \times [0,T], \tag{1a}$$

$$l_\Gamma u = \phi, \quad \text{on} \quad \partial\Omega \times [0,T], \tag{1b}$$

$$u|_{t=0} = \partial u/\partial t|_{t=0} = 0, \tag{1c}$$

where c is the speed of light. The boundary condition (1b) is inhomogeneous. For example, if u is the field scattered off a given shape Ω, then the operator l_Γ defines the type of scattering on $\partial\Omega$ and the data ϕ represent the impinging field.

The numerical method we introduce for solving the IBVP (1) combines the flexibility and ease of finite differences with the advantages of a boundary approach. It reduces the dimension of the problem by one and handles non-conforming boundaries $\partial\Omega$ on regular structured grids with no deterioration of accuracy and no adverse effect on stability due to the cut cells. These features are enabled by the method of difference potentials (MDP) [1] that employs discrete counterparts of Calderon's operators. The MDP has previously been used for the simulation of both time-harmonic [2], [3] and time-dependent waves [4]. As an extension of [4], the current work addresses exterior scattering problems. It offers high order accuracy and sub-linear computational complexity.

A fundamental difficulty in applying the boundary methods (e.g., those based on retarded potential boundary integral equations [5] or those based on Calderon's operators) to time-dependent problems is that the boundary extends as the time elapses. To avoid the associated growth of cost, we employ the strong Huygens' principle that helps us truncate the ever expanding "tail" of the algorithm. It also guarantees that only outgoing waves will be present in the solution to the exterior problem. The time marching is therefore performed on a sliding window of fixed duration and only along the boundary $\partial\Omega \times [0,T]$, which has dimension (2+1) in space-time. The reduction of the dimension translates into sub-linear complexity, so that the method outperforms the typical explicit schemes in long-time simulations. Moreover, changing the boundary condition (1b) incurs only a minor additional cost compared to that for a conventional volumetric time-stepping technique.

Work supported by US ARO, grant No. W911NF-16-1-0115, and US–Israel BSF, grant No. 2014048.

II. Method

The MDP reduces the PDE (1a) from its unbounded domain $\mathbb{R}^3\backslash\Omega \times [0,T]$ to the operator equation at the boundary $\Gamma = \partial\Omega \times [0,T]$:

$$\boldsymbol{P}_\Gamma \boldsymbol{\xi}_\Gamma = \boldsymbol{\xi}_\Gamma. \tag{2}$$

Equation (2) is known as Calderon's boundary equation with projection (BEP). In (2), $\boldsymbol{P}_\Gamma$ is a Calderon's projection for the d'Alembert operator defined as follows. Let $\boldsymbol{\xi}_\Gamma \equiv (\xi_0, \xi_1)$ be a vector function at the boundary Γ. The generalized Calderon's potential with density $\boldsymbol{\xi}_\Gamma$ is given by

$$\boldsymbol{P}_\Omega \boldsymbol{\xi}_\Gamma = \int_\Gamma \Big\{ \xi_1(\boldsymbol{y},t') G(\boldsymbol{x}-\boldsymbol{y}, t-t') - \xi_0(\boldsymbol{y},t') \frac{\partial G}{\partial \boldsymbol{n}}(\boldsymbol{x}-\boldsymbol{y}, t-t') \Big\} dt' dS_y, \tag{3}$$

where $G(\boldsymbol{x},t)$ is the fundamental solution of the d'Alembert operator. The projection $\boldsymbol{P}_\Gamma$ in (2) is the vector trace of the potential (3): $\boldsymbol{P}_\Gamma \boldsymbol{\xi}_\Gamma = \big(\boldsymbol{P}_\Omega \boldsymbol{\xi}_\Gamma, \frac{\partial \boldsymbol{P}_\Omega \boldsymbol{\xi}_\Gamma}{\partial \boldsymbol{n}}\big)\big|_\Gamma$.

The boundary equation (2) is equivalent to (1a). Namely, the function $u = u(\boldsymbol{x},t)$ provides a solution to equation (1a) if and only if its trace $\boldsymbol{\xi}_\Gamma = (\xi_0, \xi_1) \equiv \big(u, \frac{\partial u}{\partial \boldsymbol{n}}\big)\big|_\Gamma$ satisfies (2).

The BEP (2) is combined with the boundary (1b) and the two equations are solved as a system. The boundary condition (1b) can be arbitrary as long as the overall formulation (1) is well-posed. In simple cases, the boundary condition explicitly specifices one component of $\boldsymbol{\xi}_\Gamma$, e.g., ξ_0 for a Dirichlet BC and ξ_1 for a Neumann BC. The remaining component is then obtained as a solution to the BEP (2).

To discretize the BEP (2), the MDP introduces a finite difference counterpart to the projection operator $\boldsymbol{P}_\Gamma$. It is computed by solving a series of inhomogeneous auxiliary problems

978-1-7335096-2-6

(APs) for equation (1a). The AP is originally formulated as a Cauchy problem and then truncated to a bounded domain Ω_0 of simple shape, see Fig. 1, where it can be easily integrated by any appropriate finite difference scheme, for example, the compact fourth order accurate scheme [6] constructed on the Cartesian grid. A key feature of the MDP is that the non-conforming boundary $\partial\Omega$ does not lead to any loss of accuracy. Moreover, the Huygens' principle combined with the MDP enables a perfectly reflectionless treatment of the artificial outer boundary $\partial\Omega_0$, as in [7].

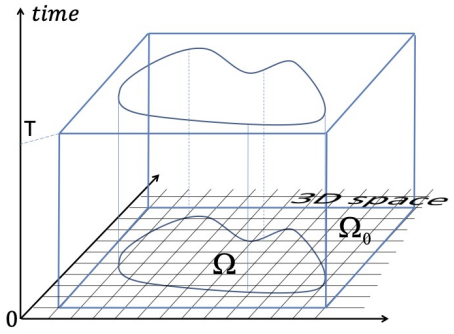

Fig. 1. Computational domain for the AP.

Furthermore, the Huygens' principle incorporated into our time-marching algorithm implies that for a bounded domain Ω in space, the extent of the backward dependence of the solution u on time is finite and non-increasing. This property allows us to solve the BEP (2) (and thus, system (1)) over long computational times $T_{\text{final}} \gg T$ sequentially, updating the density $\boldsymbol{\xi}_\Gamma$ by "chunks" of size T, see Fig. 2. Our implementation relies on the manifestation of the Huygens' principle via lacunae of the solution, i.e., voids behind aft fronts of the waves [8]. Lacunae allow us to limit the backward dependence of the MDP algorithm in time and thus solve the AP only over a finite non-increasing time interval. The latter depends on the size of the scatterer and speed of propagation, but does not depend on the frequency/wavelength. Hence, the cost of computing the solution on Γ per unit time appears fixed and non-increasing regardless of the overall simulation time. This cost scales as $\propto h^{-3}$, where h is the grid size, whereas for a conventional volumetric time-marching scheme that involves three space directions and time it would scale as $\propto h^{-4}$ (Section III). The solution u on Ω is computed only once, at $t = T_{\text{final}}$ [9].

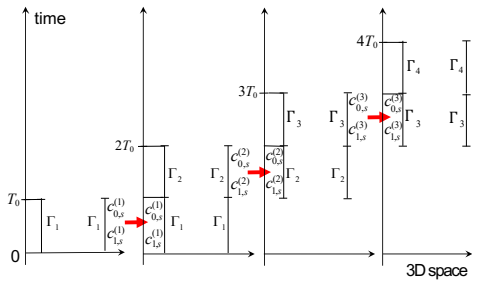

Fig. 2. Time marching by "chunks" of size T.

III. Numerical Demonstrations

To solve the AP, we employed a fourth order accurate compact scheme [6] (it controls the dispersion error more efficiently than the previously used lower order schemes). The first test case is scattering of a plane wave about a sphere of radius R_0. All computations are conducted on a Cartesian grid, for which the spherical boundary $r = R_0$ is non-conforming. Fig. 3 shows the error profiles for a long-time run with $T_{\text{final}} = 4000R_0/c$ on two consecutive grids. Table I demonstrates that the CPU time to advance the solution over $T = R_0/c$ scales roughly as $2^3 = 8$ for the proposed boundary method versus $2^4 = 16$ for an explicit volumetric scheme.

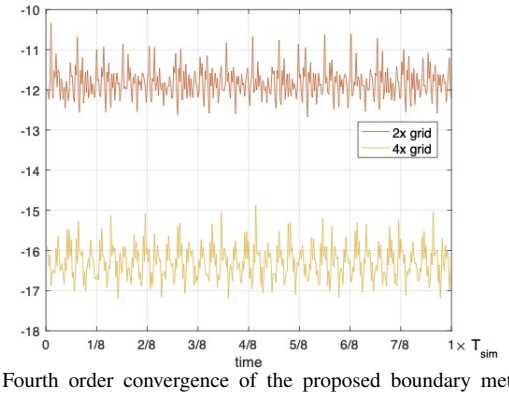

Fig. 3. Fourth order convergence of the proposed boundary method with Robin BC (1b).

TABLE I
Comparison of numerical performance over a fixed time interval $T = R_0/c$ of the proposed boundary method (MDP+lacunae) vs. standard volumetric time marching.

Grid	Volumetric Method		MDP+lacunae	
	CPU time, sec	scaling	CPU time, sec	scaling
1×	1.26	-	$6.14 \cdot 10^{-2}$	-
2×	19.8	15.7	$5.16 \cdot 10^{-1}$	8.44
4×	322	16.3	4.44	8.61

Fig. 4 shows scattering about a prolate spheroid for two different angles of incidence. Changing the angle of incidence amounts only to changing the boundary condition (1b). Therefore, all simulations in Fig. 4 are conducted without having the recompute the discrete Calderon's projection.

Yet another test case is the scattering of an impinging plane wave about a toroidal surface. The results are presented in Fig. 5.

References

[1] V. S. Ryaben'kii, *Method of Difference Potentials and Its Applications*, ser. Springer Series in Computational Mathematics. Berlin: Springer-Verlag, 2002, vol. 30.

[2] M. Medvinsky, S. Tsynkov, and E. Turkel, "The method of difference potentials for the Helmholtz equation using compact high order schemes," *J. Sci. Comput.*, vol. 53, no. 1, pp. 150–193, 2012. [Online]. Available: https://doi.org/10.1007/s10915-012-9602-y

[3] ——, "High order numerical simulation of the transmission and scattering of waves using the method of difference potentials," *J. Comput. Phys.*, vol. 243, pp. 305–322, 2013. [Online]. Available: https://doi.org/10.1016/j.jcp.2013.03.014

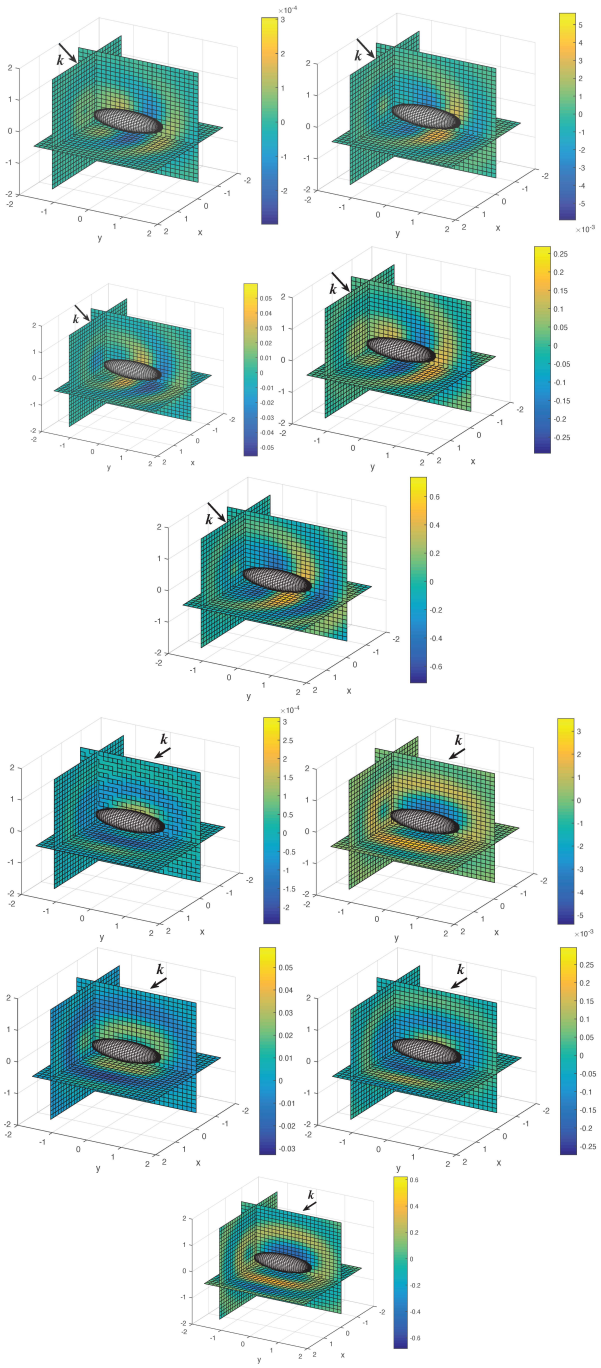

Fig. 4. 3D time-dependent scattering about a prolate spheroid for two different incident directions. The surface is parameterized using spheroidal coordinates (see [10, Volume 1]).

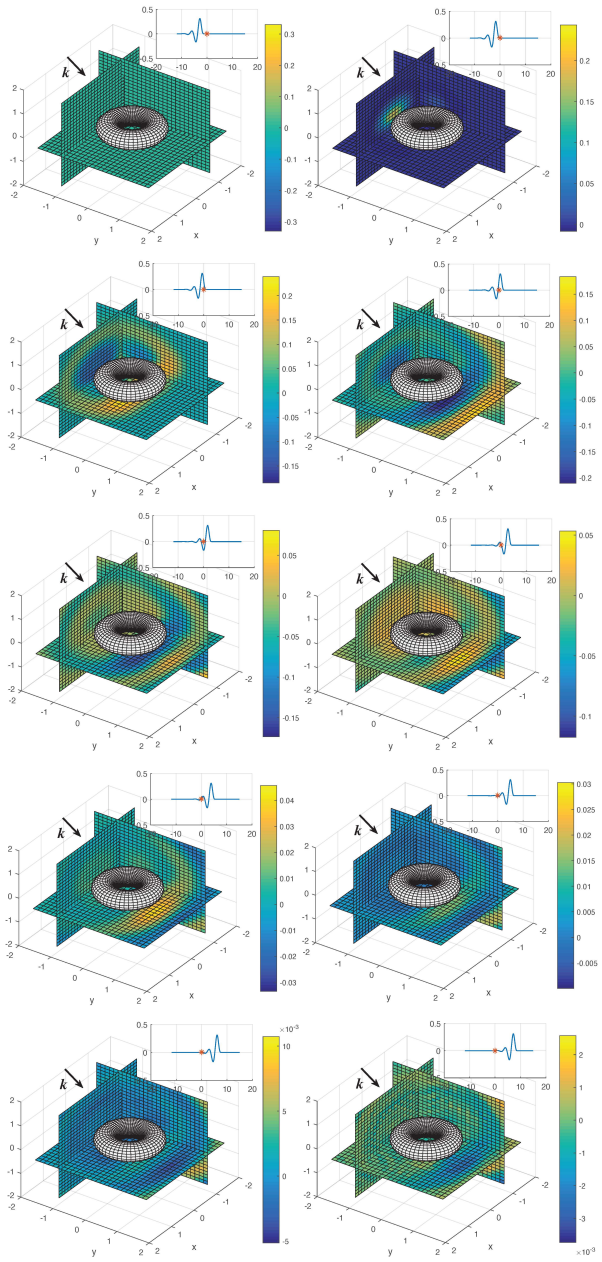

Fig. 5. 3D time-dependent scattering of a Gaussian modulated chirp about a torus. Chirp length $\sim$ torus size. The surface is represented using toroidal coordinates (see [10, Volume 1]).

[4] S. Petropavlovsky, S. Tsynkov, and E. Turkel, "A method of boundary equations for unsteady hyperbolic problems in 3D," *J. Comput. Phys.*, vol. 365, pp. 294–323, July 2018. [Online]. Available: https://doi.org/10.1016/j.jcp.2018.03.039

[5] F.-J. Sayas, *Retarded Potentials and Time Domain Boundary Integral Equations. A Road Map*, ser. Springer Series in Computational Mathematics. Cham, Switzerland: Springer, 2016, vol. 50. [Online]. Available: http://doi.org/10.1007/978-3-319-26645-9

[6] F. Smith, S. Tsynkov, and E. Turkel, "Compact high order accurate schemes for the three dimensional wave equation," *J. Sci. Comput.*, vol. 81, no. 3, pp. 1181–1209, December 2019. [Online]. Available: https://doi.org/10.1007/s10915-019-00970-x

[7] S. Petropavlovsky and S. Tsynkov, "Non-deteriorating time domain numerical algorithms for Maxwell's electrodynamics," *J. Comput. Phys.*, vol. 336, pp. 1–35, May 2017. [Online]. Available: https://doi.org/10.1016/j.jcp.2017.01.068

[8] I. Petrowsky, "On the diffusion of waves and the lacunas for hyperbolic equations," *Matematicheskii Sbornik (Recueil Mathématique)*, vol. 17 (59), no. 3, pp. 289–370, 1945.

[9] S. Petropavlovsky, S. V. Tsynkov, and E. Turkel, "Numerical solution of 3D exterior unsteady wave propagation problems using boundary operators," *SIAM J. Sci. Comput.*, vol. 42, no. 5, pp. A3462–A3488, 2020. [Online]. Available: https://doi.org/10.1137/19M1269269

[10] P. M. Morse and H. Feshbach, *Methods of Theoretical Physics. 2 Volumes*, ser. International Series in Pure and Applied Physics. New York: McGraw-Hill Book Co., Inc., 1953.